

## **D1.1. Protocol of synthesis of reference MNPLs together with their respective characterization**

---

<b>Num</b>	<b>Title</b>	<b>Due date</b>	<b>Responsible</b>	<b>Dissem Level</b>
D1.1	Protocol of synthesis of reference MNPLs together with their respective characterization	31/03/22	AIMPLAS	<b>Public</b>

---

The objective of the report is to show the work carry out in WPI to obtain MNPLs reference materials. Due to the large number of MNPLs that must be obtained, the report only summarizes what was done in the period but it will be a live deliverable since it will be necessary to add more information as progress is made in obtaining the rest of the reference materials.

---





**Index:**

- 1. Objectives.**
- 2. MNPLs obtained.**
- 3. Protocol of functionalization (AIMPLAS)**
- 4. PLA and PET nanoparticles (AIMPLAS)**
- 5. Labelling of PLA (AIMPLAS)**
- 6. PET Nanoparticles (UAB).**
- 7. Future work.**
- 8. References**





## 1. Objectives:

- To define the necessary protocols to produce the MNPLs (labelled and non labelled) defined in the project proposal.
- To carry out the necessary characterization of the MNPLs obtained.
- To study different options to stabilize suspensions obtained.
- To obtain and distribute the MNPLs obtained to the consortium.
- To define futures steps.

## 2. MNPLs obtained.

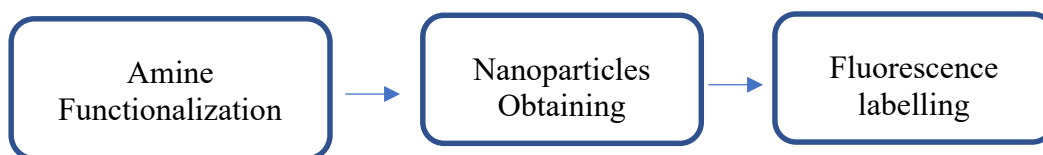
The MNPLs available for the project consortium are:

- **NanoPLA (labelled and non labelled):** obtained by AIMPLAS) in suspension.
- **Microparticles** of PP, HDPE, LDPE, PLA, PA and PET (obtained by AIMPLAS) in powder. Different sizes. Optimizations are needed to decrease the size up to 10 microns
- **NanoPET** (obtained by UAB) in suspension.

## 3. Protocol of functionalization.

To obtain labelled nanoparticles a functionalization step has been carry out. In the following scheme is showed the strategy:

### General strategy to obtain fluorescence labelled MNPLs



The protocol is divided in two steps:

- 1) Amine Functionalization (PLA, PET y PP)
- 2) Fluorescence labelling (de PLA)

The different targets of PLASTICHEAL require *ad hoc* design of new materials. In this context, functionalized polymers obtained through reactive extrusion play a role of paramount importance, allowing the chemical embedding of markers specifically



This project has received funding from the European Union's Horizon 2020 research and innovation programme under grant agreement No. 965196

## plasticheal

developed for the monitoring of MNPLs in the environment and in human beings, preventing the loss of the luminescent marker in the biological media.

The reactive extrusion is a recently developed process that allows to obtain chemically grafted polymers without the use of solvents. Despite its wide employment in industrial fields, it is gaining a considerable interest also in academic studies thanks to its applicability with thermoplastic polymers. This technique allows to perform chemical reactions between polymers and monomers or additives in the molten state. The reaction is carried out in single/twin screw extruders or torque rheometers through a continuous process with short residence times and high temperatures.

Polymers of different nature were extruded in a laboratory extruder (Figure 1) the presence of a radical initiator together with different kinds of additives presenting reactive double bonds and appropriated functional groups to functionalize the polymeric chains. Those functional groups would be either amines or carboxylic acid moieties (Figure 2) which would react with commercially available substituted fluorophores in a later stage.



Figure 1. Laboratory extruder HAAKE™ MiniLab II Micro Compounder.

### 3.2 Functionalization of polyethylene terephthalate (PET)

#### a) Grafted PET for reaction with acid-reactive fluorophores.

Some trials were done to identify the best quantity of polymer and other parameters (such as temperature and screw rate) to use. The best conditions were kept for further trials.



# plasticheal

First trials were conducted using virgin PET as polymeric matrix and different quantity of initiator and allylamine (AA) as additive (Figure 2). Purification of the extruded polymers was performed with an internal protocol.

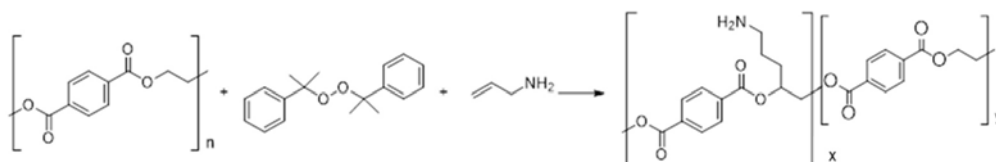


Figure 2. Functionalization of PET with Allylamine

A similar study was carried out for the grafting of oleylamine (OA) (Figure 3). The yields were in all cases above 86 %.

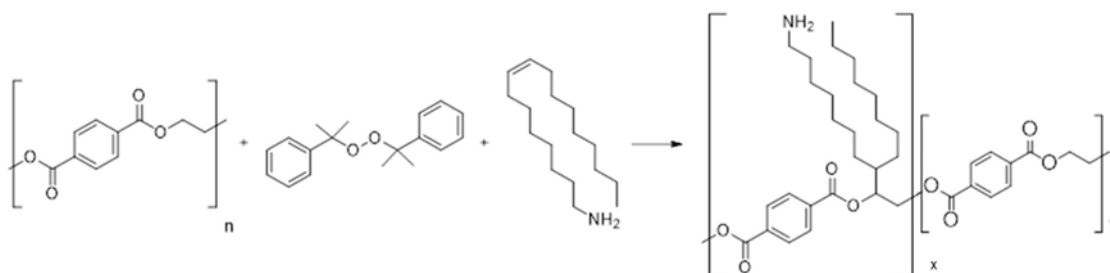


Figure 3. Functionalization of PET with Oleylamine

The successful functionalization was confirmed by the  $^1\text{H}$  NMR (nuclear magnetic resonance) spectrum recorded in  $\text{C}_2\text{D}_2\text{Cl}_4$ . The oleylamine-functionalized PET shows, besides the intense singlets at 4.68 and 8.09 ppm related to the methylene and aromatic hydrogen atoms of common PET, other signals between 8.05 and 7.79 ppm. These resonances cannot be attributed to free oleylamine but are probably related to aromatic rings close to functionalized methylene groups. Similar considerations are possible for the O-bonded CH. It is likely to suppose that resonances in the 4.48 - 3.41 ppm range are related to functionalized fragments of the polymer chains. The aliphatic resonances of the oleylamine branches are comprised between 2.01 and 0.85 ppm (Figure 4).



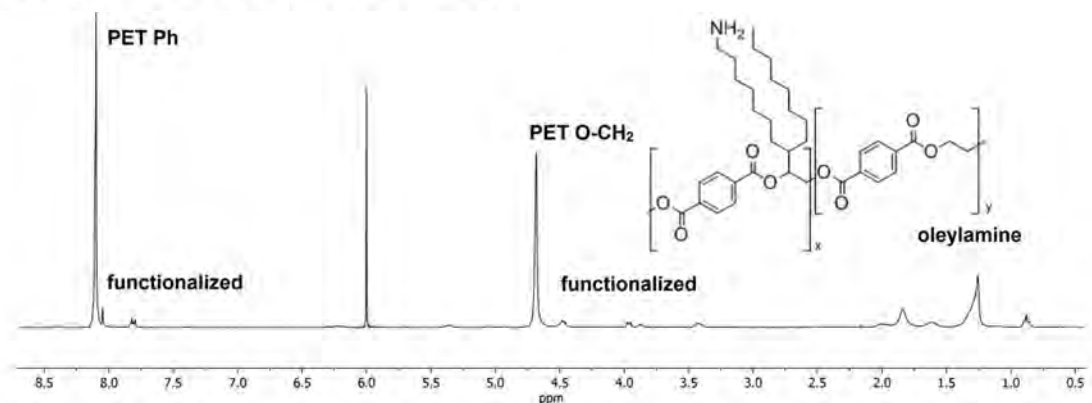


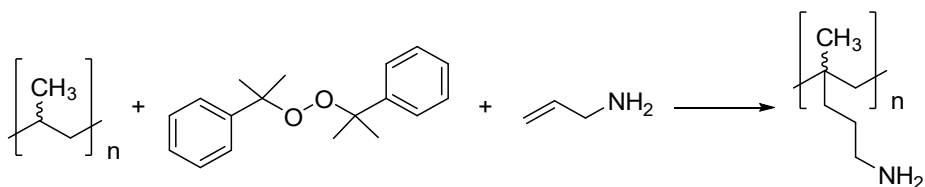
Figure 4.  $^1\text{H}$  NMR spectrum of oleylamine grafted PET (PHL-2B).  $\text{C}_2\text{D}_2\text{Cl}_4$ , 298 K.

### B) Grafted PET for reaction with amine-reactive fluorophores.

In this case, PET was reacted with other additives (Figure 5) to achieve the functionalization. Unfortunately, the desired reaction was not obtained and therefore grafting with alkenylamines was the strategy of choice for the project. Since reaction with an acid-reactive fluorophore would be easier for an oleylamine functionalized polymer rather than an allylamine grafted one, the synthesis of oleylamine substituted polymers was selected for the next steps.

### 3.3 Functionalization of polypropylene (PP). Preliminary results.

Using HAAKE, some trials were done to identify the best quantity of polymer and other parameters (as temperature and rpm of screws) to use.



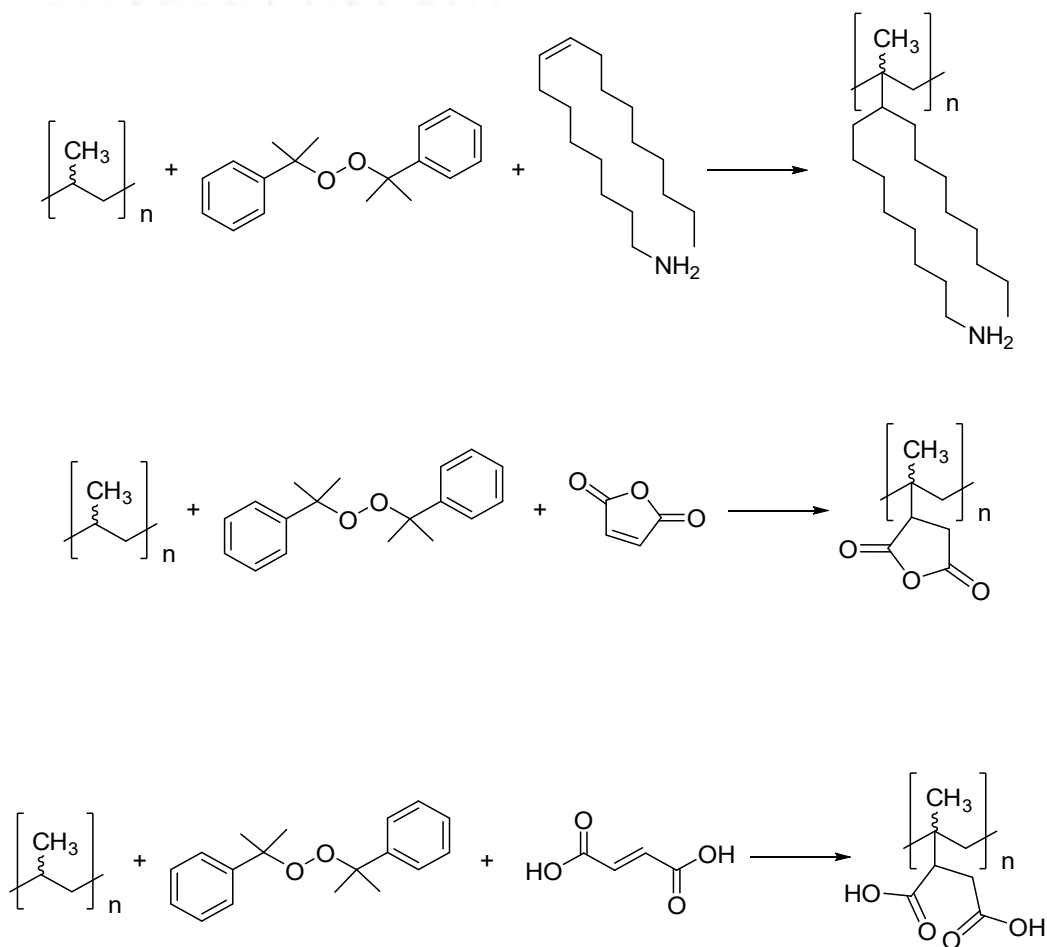


Figure 5. Functionalization of PP with different molecules.

### 3.4 Functionalization of polylactic acid (PLA)

The best conditions for these experiments were fixed. The reactions were performed in the presence of alkenylamines, *i.e.* AA and OA. The extruded was purified following an internal protocol.

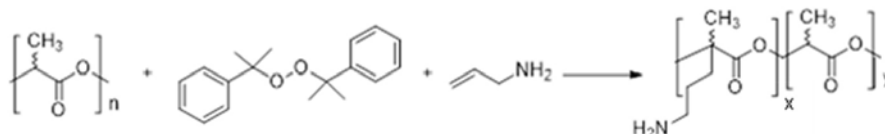


Figure 6. Functionalization of PLA with Allylamine.



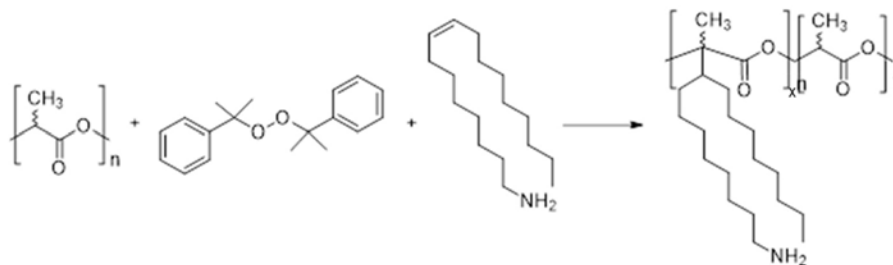


Figure 7. Functionalization of PLA with Oleylamine.

#### 4. PLA and PET nanoparticles (AIMPLAS)

##### 4.1. Nanoprecipitation of PLA

There are different methods for obtaining PLA nanoparticles. One of the most described methods in the literature for the use of PLA as a biocompatible material for the transport and release of drugs is emulsion nanoprecipitation<sup>1-14</sup>.

Using this method, it is possible to obtain nanoparticles with a low polydispersity. The method used consisted in the use of an organic phase composed of dichloromethane (DCM) and PLA and an aqueous phase composed of water and SDS as a surfactant.

The obtained nanoparticles have been characterized by **SEM and DLS. Zeta potential** has also been measured.

In a final step, as is showed in Figure 8, emulsion was pass thru a 0.45 microns filter disc. In the DLS results is showed the disappearance of the bigger one size distribution microparticles.





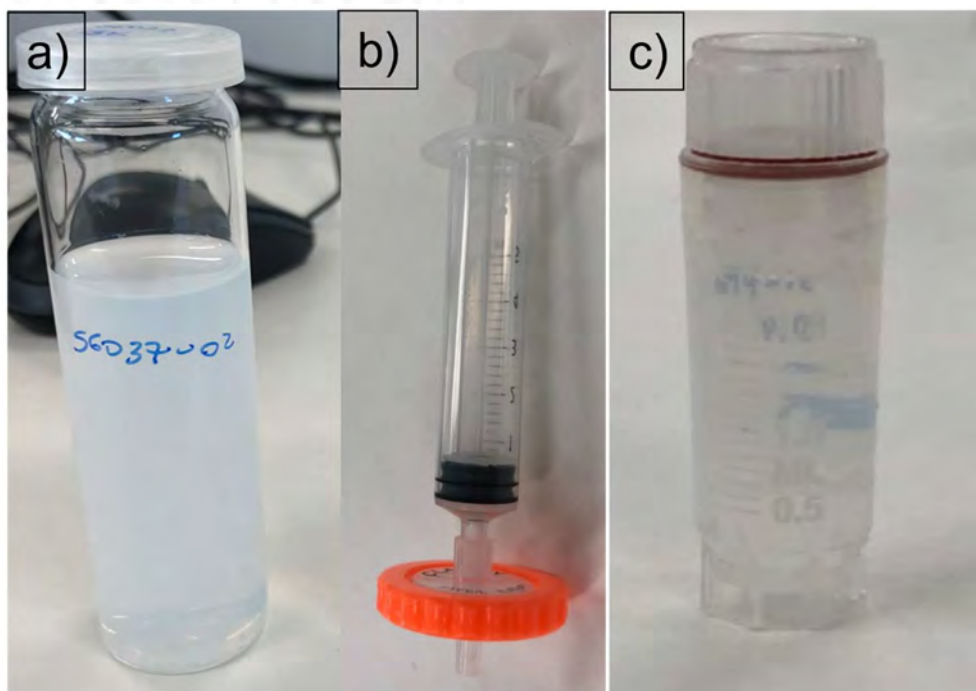


Figure 9. PLA emulsion after purification (a), filter used (b) and final purified product (c)

#### 4.2. PLA characterization.

Morphology was characterized by SEM. Water-emulsion PLA nanoparticles was characterized under electronic microscopy. In Figure 10 is showed a micrography of the obtained NPs. It is observable a distribution of sizes form nanoparticles to microparticles.



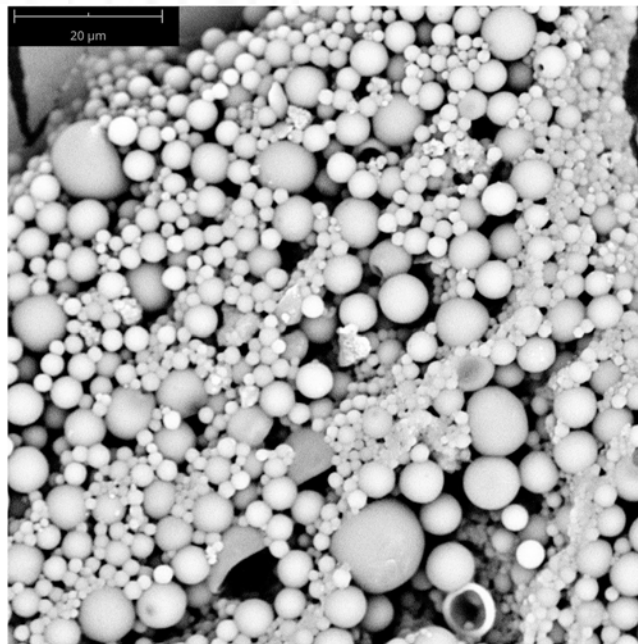


Figure 10. SEM Micrography of PLA nanoparticles as prepare

After purification with centrifuge methods, bigger nanoparticles were separated, and it is visible in the micrograph showed in Figure 11. Due the resolution of the equipment, was not possible go closer in the sample. Furthermore, with the electron beam at this work distance, sample was going to melt. This effect is visible in the Figure 12 where the functionalized nanoparticles are shown.



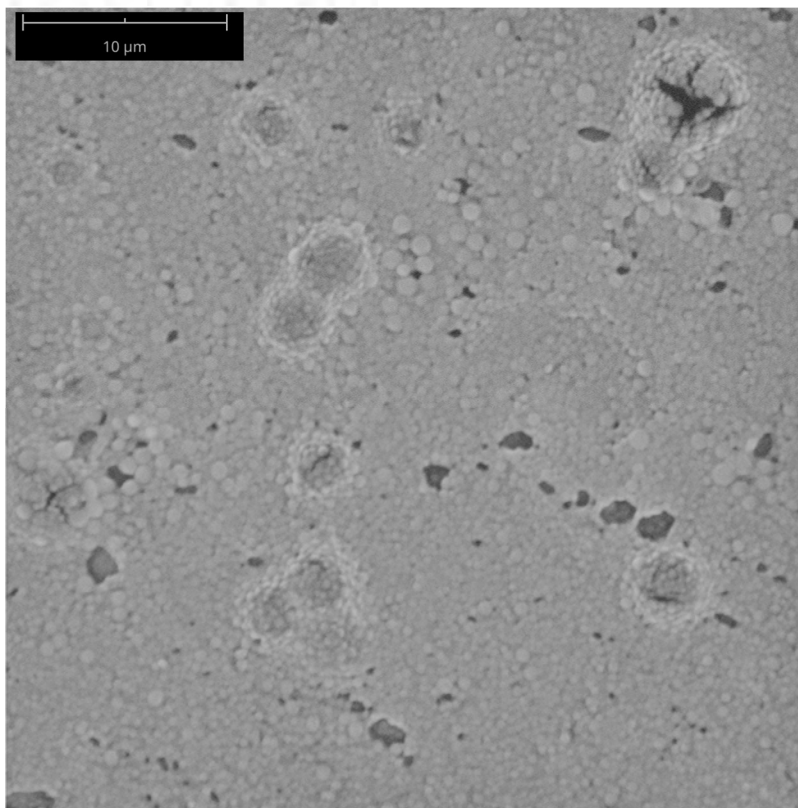


Figure 11. SEM Micrograph of the purified PLA nanoparticles

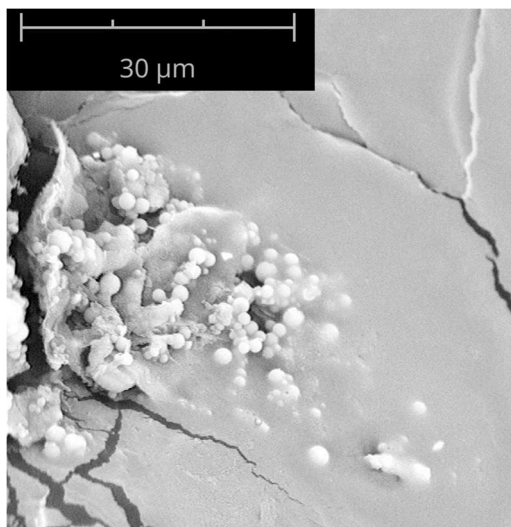


Figure 12. SEM Micrograph of the functionalized PLA-PHL12B nanoparticles

To evaluate the polydispersity of the nanoparticles, dynamic light scattering (DLS) was used. A sample was measured after removing the SDS by centrifugal cleaning (Figure 13) and after passing the sample through a 0.45-micron disc filter (Figure 14). It can be



This project has received funding from the European Union's Horizon 2020 research and innovation programme under grant agreement No. 965196



observed that the Pdl decreases considerably (0,157 vs 0.062) and the population of particles that appears in Figure 13 in the micron range disappears.



Figure 13. Size distribution of the PLA nanoparticles after SDS cleaning





**Sample Name:** SG037-2-Filtered 1  
**SOP Name:** mansettings.nano  
**File Name:** SG037-2-Filtered.dts  
**Record Number:** 1  
**Material RI:** 1,33  
**Material Absorbtion:** 0,010  
**Dispersant Name:** Water  
**Dispersant RI:** 1,330  
**Viscosity (cP):** 0,8872  
**Measurement Date and Time:** martes, 15 de marzo de 2022 12:19:...

**Temperature (°C):** 25,0  
**Count Rate (kcps):** 192,2  
**Cell Description:** Disposable sizing cuvette  
**Duration Used (s):** 32  
**Measurement Position (mm):** 4,65  
**Attenuator:** 7

	Size (d.nm):	% Intensity:	St Dev (d.nm):
<b>Z-Average (d.nm):</b> 137,7	<b>Peak 1:</b> 146,8	100,0	36,42
<b>Pdl:</b> 0,062	<b>Peak 2:</b> 0,000	0,0	0,000
<b>Intercept:</b> 0,951	<b>Peak 3:</b> 0,000	0,0	0,000

**Result quality :** Good

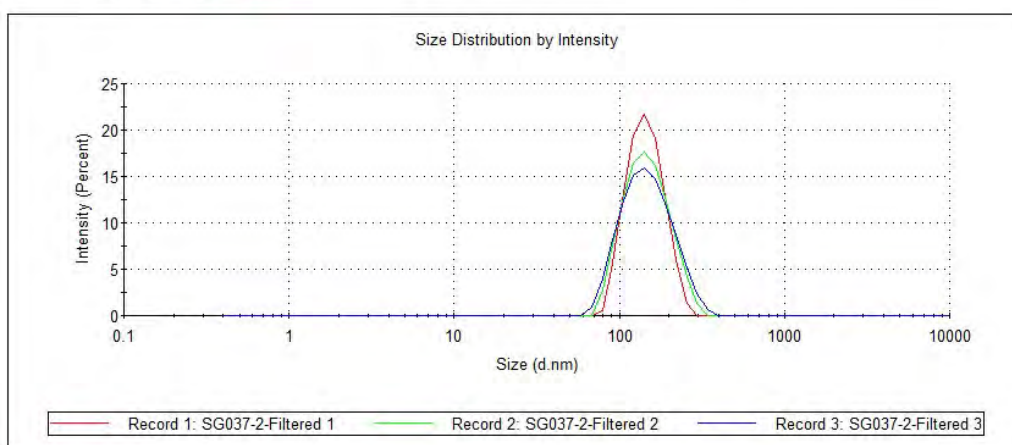


Figure 14. Size distribution of the PLA nanoparticles after SDS cleaning and filtering by 0.45-micron filter disc

The plot of intensity (%) versus sample size (nm) of functionalized PLA-PHL12B is shown in Figure 15. Values obtained were like the previous PLA nanoparticles without functionalization with a Pdl values of 0,089.

Results for the Fluorescein labelled PLA are shown in the Figure 16. With Pdl of 0.031 were the lower Z-Average (105,9 nm).







**Sample Name:** SG029.1  
**SOP Name:** mansettings.nano  
**File Name:** 220210.dts  
**Record Number:** 6  
**Material RI:** 1,59  
**Material Absorbtion:** 0,010  
**Dispersant Name:** Water  
**Dispersant RI:** 1,330  
**Viscosity (cP):** 0,8872  
**Measurement Date and Time:** jueves, 10 de febrero de 2022 14:18:..

**Temperature (°C):** 25,0  
**Count Rate (kcps):** 406,1  
**Cell Description:** Disposable sizing cuvette  
**Duration Used (s):** 32  
**Measurement Position (mm):** 4,65  
**Attenuator:** 5

	Size (d.nm):	% Intensity:	St Dev (d.nm):
<b>Z-Average (d.nm):</b> 105,9	<b>Peak 1:</b> 118,5	100,0	38,86
<b>PdI:</b> 0,089	<b>Peak 2:</b> 0,000	0,0	0,000
<b>Intercept:</b> 0,925	<b>Peak 3:</b> 0,000	0,0	0,000
<b>Result quality :</b> Good			

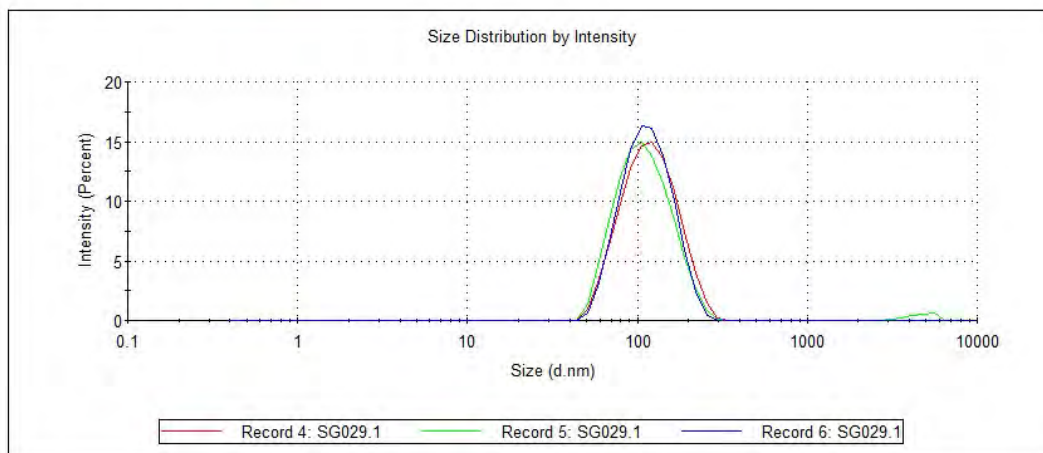


Figure 15. Size distribution of the functionalized PLA-PHL12B nanoparticles after SDS cleaning





**Sample Name:** SG050-F  
**SOP Name:** mansettings.nano  
**File Name:** 220309.dts  
**Record Number:** 12  
**Material RI:** 1,59  
**Material Absorbtion:** 0,010  
**Dispersant Name:** Water  
**Dispersant RI:** 1,330  
**Viscosity (cP):** 0,8872  
**Measurement Date and Time:** miércoles, 9 de marzo de 2022 17:0...

**Temperature (°C):** 25,0  
**Count Rate (kcps):** 369,4  
**Cell Description:** Disposable sizing cuvette  
**Duration Used (s):** 32  
**Measurement Position (mm):** 4,65  
**Attenuator:** 9

	Size (d.nm):	% Intensity:	St Dev (d.nm):
<b>Z-Average (d.nm):</b> 136,1	<b>Peak 1:</b> 143,1	100,0	33,39
<b>PdI:</b> 0,031	<b>Peak 2:</b> 0,000	0,0	0,000
<b>Intercept:</b> 0,929	<b>Peak 3:</b> 0,000	0,0	0,000
<b>Result quality :</b> Good			

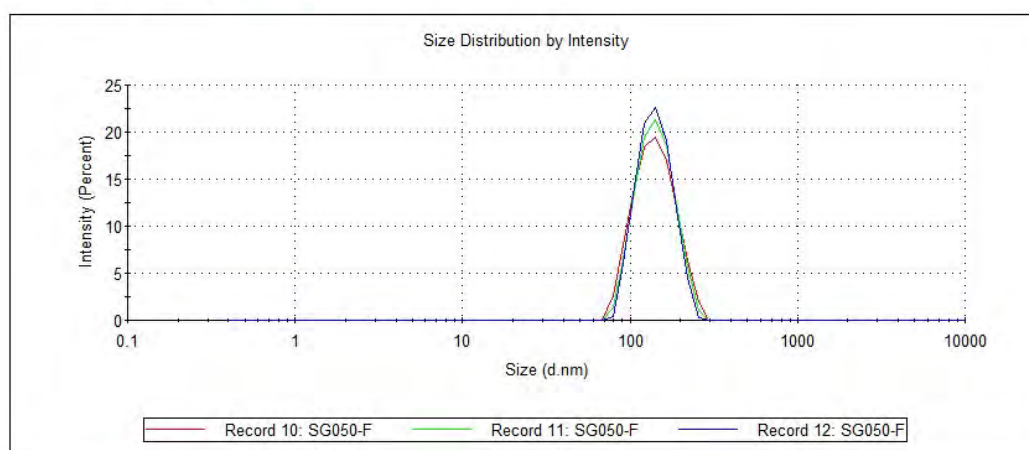


Figure 16. Size distribution of the Fluorescein labelled PLA nanoparticles after SDS cleaning and filtering

The stability of the emulsion was evaluated using Zeta potential and is estimated by measuring electrophoretic mobility of the droplets. Zeta potential is often used as an indicator of the droplet stability, where values more positive than +30 mV and more negative than -30 mV indicate good stability against coalescence<sup>15</sup>.

Zeta potential distribution of the PLA nanoparticles before and after filtration with 0,45 filter disc, are shown in Figure 17 and 18 respectively. Results obtained for functionalized PLA-PHL15A and Fluorescein labelled PLA are shown in Figure 19 and Figure 20.

In the case of PLA nanoparticles, similar values were obtained before and after filtration of the samples, with a Zeta Potential of -41 mV and -48 mV respectively.





Measurement of functionalized PLA-PHL15A nanoparticles was not with enough quality. Probably was because the measurement was done 2 weeks after preparation and flocculation process started.



Figure 17. Zeta potential distribution of the PLA nanoparticles







**Sample Name:** SG037-2-Filtered\_Zeta\_b 1  
**SOP Name:** mansettings.nano  
**File Name:** SG037-2-Filtered\_Zeta.dts  
**Record Number:** 4  
**Date and Time:** martes, 15 de marzo de 2022 12:33:44  
**Dispersant Name:** Water  
**Dispersant RI:** 1,330  
**Viscosity (cP):** 0,8872  
**Dispersant Dielectric Constant:** 78,5

**Temperature (°C):** 25,0  
**Count Rate (kcps):** 177,2  
**Cell Description:** Clear disposable zeta cell  
**Zeta Runs:** 12  
**Measurement Position (mm):** 2,00  
**Attenuator:** 9

	Mean (mV)	Area (%)	St Dev (mV)
<b>Zeta Potential (mV):</b> -37,8	<b>Peak 1:</b> -37,8	100,0	8,53
<b>Zeta Deviation (mV):</b> 8,53	<b>Peak 2:</b> 0,00	0,0	0,00
<b>Conductivity (mS/cm):</b> 0,0625	<b>Peak 3:</b> 0,00	0,0	0,00

**Result quality :** Good

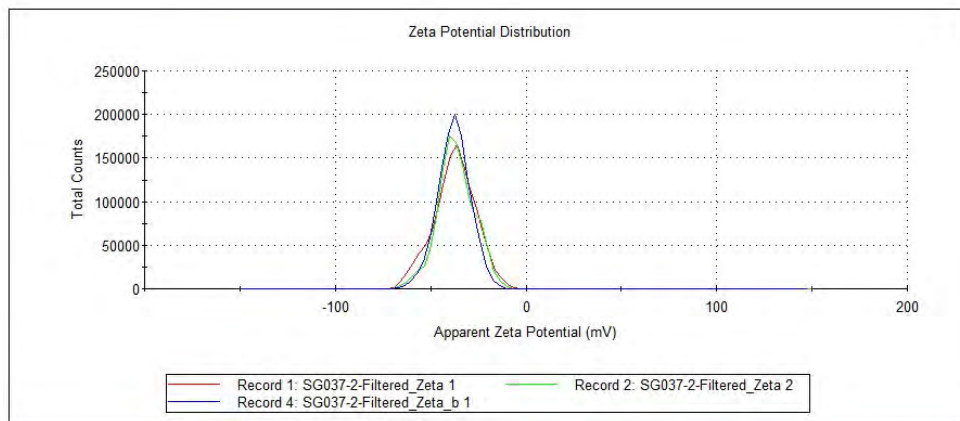


Figure 18. Zeta potential distribution of the PLA nanoparticles after SDS cleaning and filtering by 0.45-micron filter disc





Sample Name: SG050-F

SOP Name: mansettings.nano

File Name: 220309.dts

Record Number: 22

Date and Time: miércoles, 9 de marzo de 2022 17:19:33

Dispersant Name: Water

Dispersant RI: 1,330

Viscosity (cP): 0,8872

Dispersant Dielectric Constant: 78,5

Temperature (°C): 25,0

Count Rate (kcps): 60,2

Cell Description: Clear disposable zeta cell

Zeta Runs: 12

Measurement Position (mm): 2,00

Attenuator: 11

	Mean (mV)	Area (%)	St Dev (mV)
Zeta Potential (mV): -20,1	Peak 1: -19,9	98,6	9,94
Zeta Deviation (mV): 10,8	Peak 2: -52,5	1,2	2,89
Conductivity (mS/cm): 0,00844	Peak 3: 40,3	0,3	0,00

Result quality : See result quality report

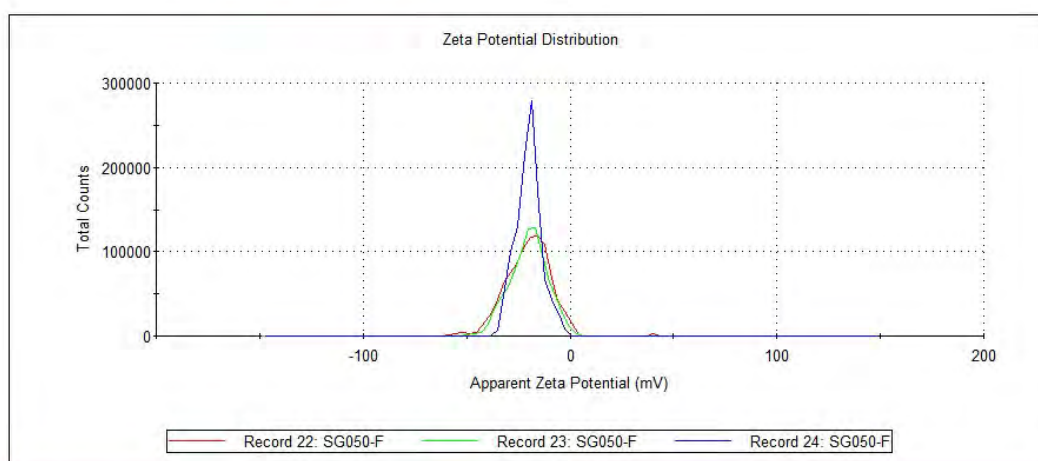


Figure 19. Zeta potential distribution of the Fluorescein labelled PLA

### 4.3. Nanoprecipitation of PET (previous trials)

Same strategy as PLA nanoparticles by emulsion precipitation was followed for the preparation of PET nanoparticles. For this polymer, dichloromethane it was not useful, so a mixture of organic solvents was used.

PET and functionalized PET was prepared by this methodology. Morphology was characterized by SEM. Results of the PET nanoparticles and functionalized PET-PHL2C, PET-PHL10A and PET-PHL2D are shown in Figures 20, Figure 21, Figure 22 and Figure 23 respectively



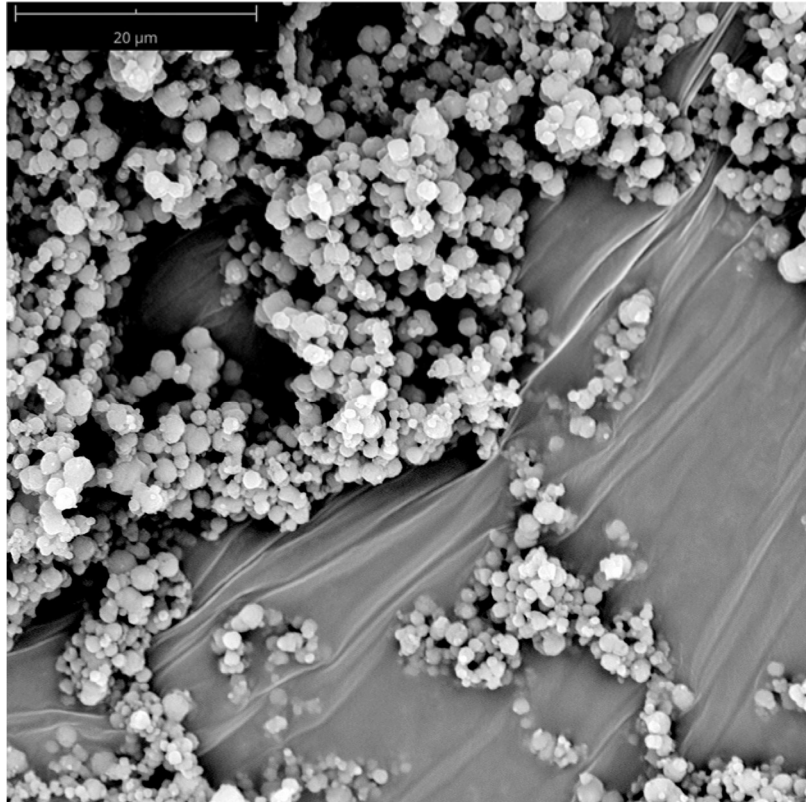


Figure 20. SEM Micrograph of PET nanoparticles



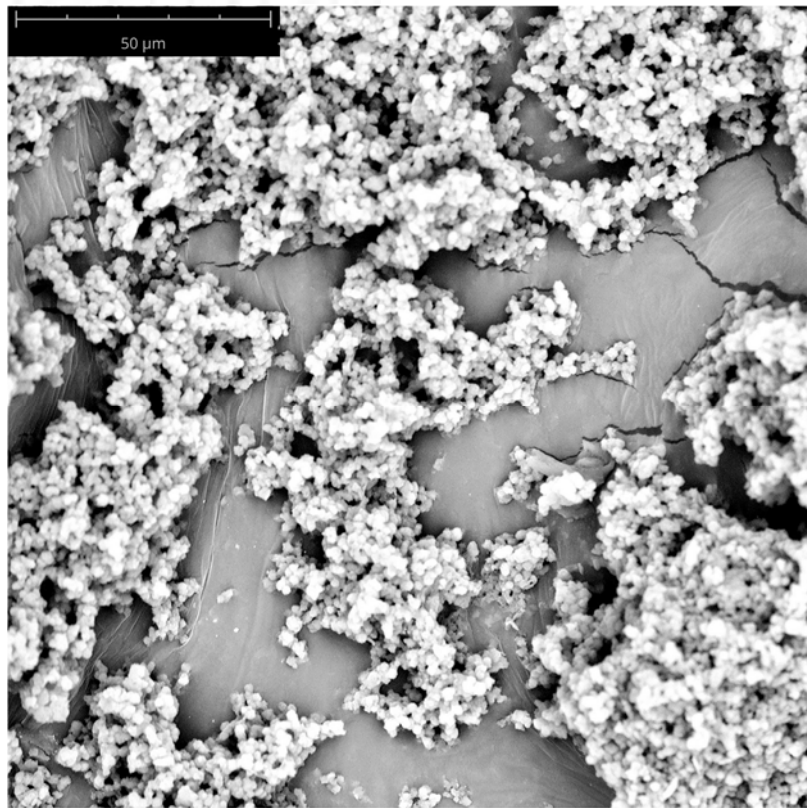


Figure 21. SEM Micrograph of functionalized PET-PHL2C nanoparticles

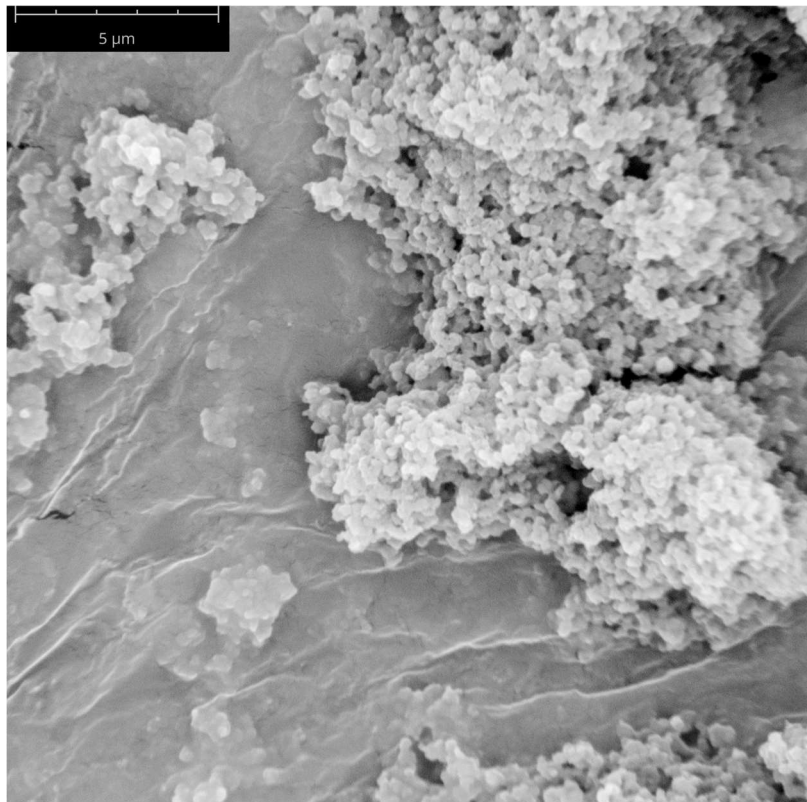




Figure 22. SEM Micrograph of functionalized PET-PHL10A nanoparticles

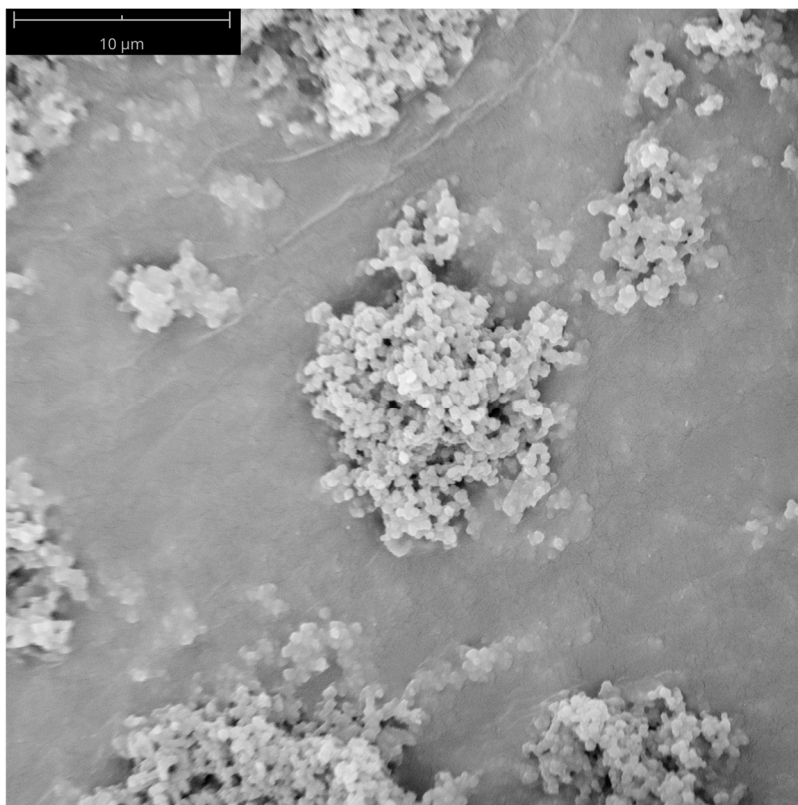


Figure 23. SEM Micrograph of functionalized PET-PHL2D nanoparticles

## 5. Labelling of PLA (AIMPLAS)

### 5.1 Labelling of PLA.

The amino-functionalized PLA nanoparticle suspensions were labeled employing 5-Carboxyfluorescein, Succinimidyl Ester (Figure 24). The succinimidyl ester moiety is very reactive towards primary amine groups as the ones present in the oleylamine grafted PLA nanoparticles.



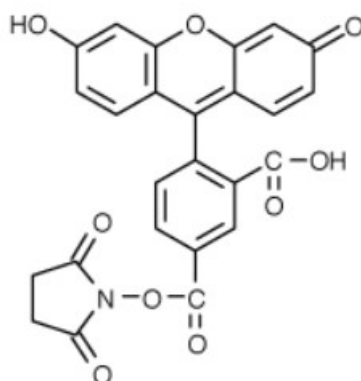


Figure 24. 5-Carboxyfluorescein, Succinimidyl Ester.

The reaction took place in the dark at room temperature for one hour. Non-reacted fluorophore was removed by ultracentrifugation.



Figure 25. reaction set-up for the fluorescent labelling of PLA nanoparticles.

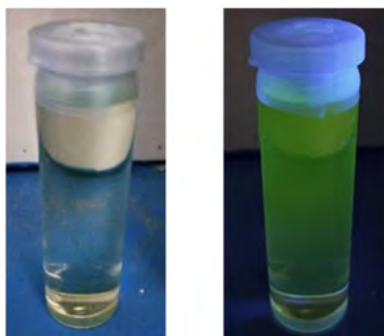


Figure 26. Fluorescein labelled PLA nanoparticle suspension (left) shows fluorescence upon irradiation with a 254 nm lamp (right).





## 5.2. Summary and future improvements

Nanoparticles of PLA, functionalized PLA and Fluorescein labelled PLA was performed by emulsion nanoprecipitation. Emulsions were stable during months (with SDS) and during weeks (suspended in water). Some trials were done with albumin and PVA as co-stabilizers.

Nanoparticles were characterized by SEM, DLS and Zeta potential. SEM micrographs showed a good size distribution and it was confirmed by DLS with values below 10% PDI and a Z-Average between 136-170 nm.

PET nanoparticles have been obtained with the same procedure as PLA nanoparticles. SEM micrographs showed a good size distribution, but stability is quite poor (only days) and needs improvements.

New formulations with other surfactants with biological compatibility are ongoing to increase the stability of both PLA and PET emulsions.

## 6. PET Nanoparticles (UAB).

### 6.1. PET nanoparticles obtaining (UAB).

The PET raw material used to produce PET-NPLs was obtained from commercially available water plastic bottles. The developed procedure was adapted from the previously reported by Rodríguez-Hernández et al. (2019). Briefly, pieces of about 12 cm<sup>2</sup> from the bottom part of the water bottles were initially sanded with aluminum oxide/silicon carbide rotary burrs. Due to the observed metal-contamination a diamond rotary burr sander accessory, attached to a flexible shaft powered by a multitool Dremel 3000, was chosen for the sanding process. The obtained PET debris was passed through a 0.2 mm sieve (CISA R-92), and 4 g of the resulting material were dispersed in 40 mL of pre-heated (50 °C) trifluoroacetic acid (TFA, 90% v/v), in a proportion of 10 mL TFA per gram of sieved PET, on a stirring plate at 100 rpm for 2 h. After a complete dispersion, the mixture was kept at room temperature overnight in continuous agitation. Next day, 40 mL of TFA 20% (v/v) was added to the sample and the mixture was kept under constant and vigorous stirring for 24 h. After that, the obtained dispersion was distributed on six 10 mL glass tubes and centrifuged at 2500 RCF for 1 h. Once the supernatants were discarded, the obtained pellets were resuspended on 400 mL of 0.5% sodium dodecyl sulfate (SDS) solution, vigorously mixed, and distributed into two 200 mL beakers, for ultrasonication on an SSE-1 Branson sonicator. Sonication lasted for 2 min at 25% amplitude, in 9/9 s



This project has received funding from the European Union's Horizon 2020 research and innovation programme under grant agreement No. 965196

# plasticheal

sonication/break cycles. The volume of each beaker was transferred to a graduated cylinder, where sedimentation of larger particles took place for 1 h. The top 100 mL of the suspension (from each graduated cylinder) was collected, resuspended, and sonicated at 10% amplitude for 16 min in a cold-water bath, aliquoted, and immediately frozen in liquid nitrogen and stored at -80 °C for further use. Each one of the cryotubes contained 1 mL of a concentration of 12.5 mg/mL.

## 6.2. PET nanoparticles characterization (UAB).

The characterization of PET nanoparticles includes:

### **Scanning Electron Microscopy / Energy Dispersive X-Ray Microscopy (SEM-EDS).**

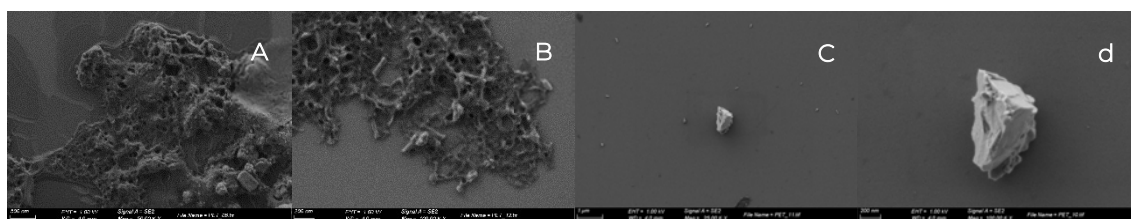


Figure. 27. **Scanning electron microscopy results.** Amorphous structures can be observed as aggregates (A) or a constituent part of a holey structure. Structures from a diverse range of geometry can be observed as aggregates (B). Single particle at the center of the field surrounded by smaller ones (C), Close up of the particle.

### **Transmission Electron Microscopy (TEM)**

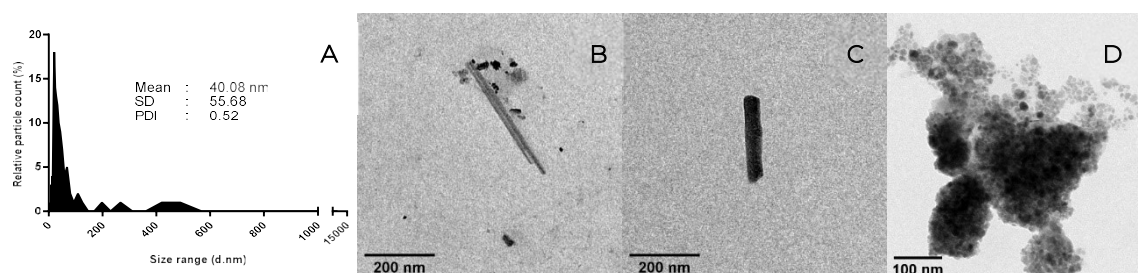


Figure 28. PET characterized by **TEM**. Size distribution of sizes was obtained from measures of more than 100 particles showing a bimodal distribution, with the main pick with sizes around 50 nm, and a second pick with sizes around 400-500 nm (A). Fields with many small sized materials and irregular shapes and fibers like structures (B). Rod-like structure (C). Aggregates permit to visualize the small sizes of their components (D).



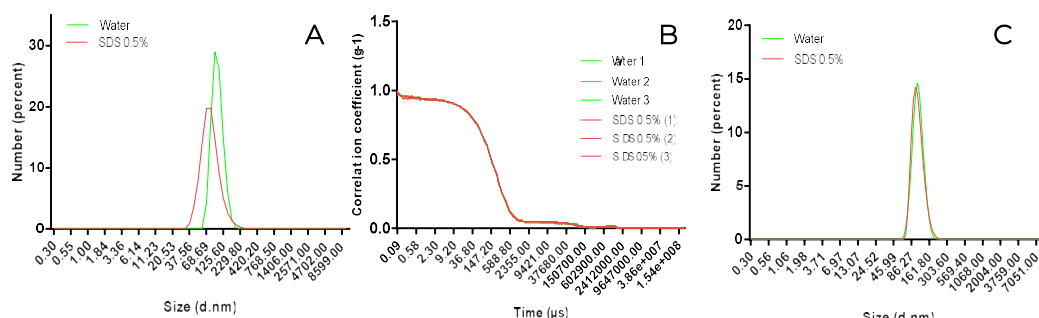


### Fourier Transform Infrared Spectroscopy (FTIR).

Assignment	Wavenumber (cm <sup>-1</sup> )
Out of plane benzene group	725 – 870
CH <sub>2</sub> rocking of glycol	845 – 897
C-O stretching of glycol	970
In plane vibration of benzene	1017
Mainly due to ester C=O stretching	1090 – 1230
CH <sub>2</sub> wagging of glycol	1340 – 1370
Benzyl ring Trans and Cis isomers ethylene segments	1410 1472 – 1440 – 1458
C=O stretching band	1714

Figure 29. FTIR spectra. Identity of principal picks of the interferogram (a) and its assignment (b). Vertical lines indicate coincident picks.

### Multi Angle and Dynamic Light scattering (DLS-MADLS) and Zeta Potential



	pH	Zeta Potential	Conductivity	Mobility	Particle concentration (particles/mL)
Water	7.10±0.21	-29.90	0.01	- 2.34±0.03	8.68x10 <sup>8</sup>
SDS (0.5%)	6.9±0.01	-35.40	0.80	- 2.78±0.05	1.19x10 <sup>9</sup>





Figure 30. Size distribution analysis by DLS. (A) Filtered and sonicated PET-NPLs samples were used with both water and SDS (0.5%) as dispersants, and 174.7 as the angle of scattering collection. (B) The correlation coefficients of the measurements. (C) Particle size distribution by using MADLS with three angles of scattering collection (174.7, 90, and 12.78) with water or SDS (0.5%) as dispersants.

## 7. Future Work.

It is necessary to continue working in the obtaining of reference materials to have available for the project at least 4 types of MNPLs and one type of nanofiber.

On going work include:

- To obtain PLA suspensions more concentrated.
- To obtain micro nanoparticles in the size of 10 microns.
- To obtain PET nanoparticles in the range of 10 microns
- To obtain micro-PET and micro-PLA labelled.
- To obtain PET nanofibers.
- To obtain PP and PE MNPLs labelled and non labelled.

As Plasticheal project is inside the CUSP cluster several meetings have been carry out to share MNPLs to have common materials for the five projects included in the cluster.



## 8. References.

- (1) Poly(D,L-Lactic Acid) Nanoparticle Size Reduction Increases Its Immunotoxicity \_ Enhanced Reader.Pdf.
- (2) Luz, C. M.; Boyles, M. S. P.; Falagan-Lotsch, P.; Pereira, M. R.; Tutumi, H. R.; Oliveira Santos, E.; Martins, N. B.; Himly, M.; Sommer, A.; Foissner, I.; Duschl, A.; Granjeiro, J. M.; Leite, P. E. C. Poly-Lactic Acid Nanoparticles (PLA-NP) Promote Physiological Modifications in Lung Epithelial Cells and Are Internalized by Clathrin-Coated Pits and Lipid Rafts. *J. Nanobiotechnology* **2017**, *15* (1), 1–18. <https://doi.org/10.1186/s12951-016-0238-1>.
- (3) Hou, Z.; Wei, H.; Wang, Q.; Sun, Q.; Zhou, C.; Zhan, C.; Tang, X.; Zhang, Q. New Method to Prepare Mitomycin c Loaded Pla-Nanoparticles with High Drug Entrapment Efficiency. *Nanoscale Res. Lett.* **2009**, *4* (7), 732–737. <https://doi.org/10.1007/s11671-009-9312-z>.
- (4) Cheng, Q.; Qin, W.; Yu, Y.; Li, G.; Wu, J.; Zhuo, L. Preparation and Characterization of PEG-PLA Genistein Micelles Using a Modified Emulsion-Evaporation Method. *J. Nanomater.* **2020**, *2020*, 1–15. <https://doi.org/10.1155/2020/3278098>.
- (5) Sousa, S.; Costa, A.; Silva, A.; Simões, R. Poly(Lactic Acid)/Cellulose Films Produced from Composite Spheres Prepared by Emulsion-Solvent Evaporation Method. *Polymers (Basel)*. **2019**, *11* (1), 1–20. <https://doi.org/10.3390/polym11010066>.
- (6) Qiao, Z.; Wang, Z.; Zhang, C.; Yuan, S.; Zhu, Y.; Wang, J. PVAm-PIP/PS Composite Membrane with High Performance for CO<sub>2</sub>/N<sub>2</sub> Separation. *AIChE J.* **2012**, *59* (4), 215–228. <https://doi.org/10.1002/aic>.
- (7) Lancheros, R. J.; Beleño, J. Á.; Guerrero, C. A.; Godoy-Silva, R. D. Producción de Nanopartículas de PLGA Por El Método de Emulsión y Evaporación Para Encapsular N-Acetilcisteína (NAC). *Univ. Sci.* **2014**, *19* (2), 161–168. <https://doi.org/10.11144/Javeriana.SC19-2.pnpm>.
- (8) Ferrari, R.; Cingolani, A.; Moscatelli, D. Solvent Effect in PLA-PEG Based Nanoparticles Synthesis through Surfactant Free Polymerization. *Macromol. Symp.* **2013**, *324* (1), 107–113. <https://doi.org/10.1002/masy.201200073>.
- (9) Chen, J. L.; Chiang, C. H.; Yeh, M. K. The Mechanism of PLA Microparticle Formation by Water-in-Oil-in-Water Solvent Evaporation Method. *J. Microencapsul.* **2002**, *19* (3), 333–346. <https://doi.org/10.1080/02652040110105373>.
- (10) Nayak, B.; Panda, A. K.; Ray, P.; Ray, A. R. Formulation, Characterization and Evaluation of Rotavirus Encapsulated PLA and PLGA Particles for Oral Vaccination. *J. Microencapsul.* **2009**, *26* (2), 154–165. <https://doi.org/10.1080/02652040802211709>.
- (11) Feng, J.; Yang, G.; Zhang, S.; Liu, Q.; Jafari, S. M.; McClements, D. J. Fabrication and Characterization of  $\beta$ -Cypermethrin-Loaded PLA Microcapsules Prepared by Emulsion-Solvent Evaporation: Loading and Release Properties. *Environ. Sci. Pollut. Res.* **2018**, *25* (14), 13525–13535. <https://doi.org/10.1007/s11356-018-1557-6>.
- (12) Zhu, K. J.; Jiang, H. L.; Du, X. Y.; Wang, J.; Xu, W. X.; Liu, S. F. Preparation and Characterization of HCG-Loaded Polylactide or Poly(Lactide-Co-Glycolide) Microspheres Using a Modified Water-in-Oil-in-Water (w/o/w) Emulsion Solvent Evaporation Technique. *J. Microencapsul.* **2001**, *18* (2), 247–260.





- <https://doi.org/10.1080/02652040010000474>.
- (13) Singh, N. A.; Mandal, A. K. A.; Khan, Z. A. Fabrication of PLA-PEG Nanoparticles as Delivery Systems for Improved Stability and Controlled Release of Catechin. *J. Nanomater.* **2017**, 2017. <https://doi.org/10.1155/2017/6907149>.
- (14) Wang, R.; Xu, Y. Development and Evaluation of Nanoparticles Based on MPEG-PLA for Controlled Delivery of Vinpocetine: In Vitro and in Vivo Studies. *Artif. Cells, Nanomedicine Biotechnol.* **2017**, 45 (1), 157–162. <https://doi.org/10.3109/21691401.2016.1138492>.
- (15) Samimi, S.; Maghsoudnia, N.; Eftekhari, R. B.; Dorkoosh, F. *Lipid-Based Nanoparticles for Drug Delivery Systems*; Elsevier Inc., 2018. <https://doi.org/10.1016/B978-0-12-814031-4.00003-9>.

